

Coupled-mode theory and propagation losses in photonic crystal waveguides

S. Olivier, H. Benisty, C. Weisbuch¹, C. J. M. Smith², T. F. Krauss³, R. Houdré⁴

¹Laboratoire PMC, Ecole Polytechnique, F-91128 Palaiseau cedex, France
also at Laboratoire Charles Fabry, Institut d'Optique, 91403 Orsay, France

²Optoelectronics Research Group, University of Glasgow, Glasgow G12 8LT, United Kingdom

³School of Astronomy, University of St. Andrews, Fife KY16 9SS, United Kingdom

⁴Institut IPEQ, Ecole Polytechnique Fédérale de Lausanne, CH-1015 Lausanne, Switzerland

hb@pmc.polytechnique.fr

Abstract: Mode coupling phenomena, manifested by transmission “mini-stopbands”, occur in two-dimensional photonic crystal channel waveguides. The huge difference in the group velocities of the coupled modes is a new feature with respect to the classical Bragg reflection occurring, e.g., in distributed feedback lasers. We show that an adequate ansatz of the classical coupled-mode theory remarkably well accounts for this new phenomenon. The fit of experimental transmission data from GaAs-based photonic crystal waveguides then leads to an accurate determination of the propagation losses of both fundamental and higher, low-group-velocity modes.

©2003 Optical Society of America

OCIS codes: (130.0130) Integrated Optics; (230.7380) Channel waveguides

References and Links

1. S. Olivier, M. Rattier, H. Benisty, C. Weisbuch, C. J. M. Smith, R. M. De La Rue, T. F. Krauss, U. Oesterle and R. Houdré, “Mini stopbands of a one dimensional system: the channel waveguide in a two-dimensional photonic crystal,” *Phys. Rev. B* **63**, 113311 (2001).
 2. S. Olivier, H. Benisty, C. J. M. Smith, M. Rattier, C. Weisbuch, T. F. Krauss, R. Houdré and U. Oesterle, “Transmission properties of two-dimensional photonic crystal channel waveguides,” *Opt. Quantum Electron.* **34**, 171-181 (2002).
 3. C. J. M. Smith, R. M. De La Rue, M. Rattier, S. Olivier, H. Benisty, C. Weisbuch, T. F. Krauss, R. Houdré and U. Oesterle, “Coupled guide and cavity in a two-dimensional photonic crystal,” *App. Phys. Lett.* **78**, 1487-1489 (2001).
 4. H. Benisty, “Modal analysis of optical guides with two-dimensional photonic band-gap boundaries,” *J. Appl. Phys.* **79**, 7483-7492 (1996).
 5. M. Qiu, “Effective index method for heterostructure-slab-waveguide-based two-dimensional photonic crystals,” *Appl. Phys. Lett.* **81**, 1163-1165 (2002).
 6. H. Kogelnick and C.V. Shank, “Coupled wave theory of distributed feedback lasers,” *J. Appl. Phys.* **43**, 2328 (1972).
 7. See for example Tamir, *Guided Wave Optoelectronics*, Springer Verlag, Berlin, chaps 2,6 (1988).
 8. P. Ferrand, R. Romestain and J.C. Vial, “Photonic band-gap properties of a porous silicon periodic planar waveguide,” *Phys. Rev. B* **63**, 115106 (2001).
 9. E. Peral and A. Yariv, “Supermodes of grating-coupled multimode waveguides and application to mode conversion between copropagating modes mediated by backward Bragg scattering,” *J. Lightwave Tech.* **17**, 942-947 (1999).
 10. D. Labilloy, H. Benisty, C. Weisbuch, T.F. Krauss, R. Houdré and U. Oesterle, “Use of guided spontaneous emission of a semiconductor to probe the optical properties of two-dimensional photonic crystals,” *Appl. Phys. Lett.* **71**, 738-740 (1997).
 11. E. Schwoob, H. Benisty, S. Olivier, C. Weisbuch, C.J.M Smith, T.F. Krauss, R. Houdre and U. Oesterle, “Two-mode fringes in planar photonic crystal waveguides with constrictions: a sensitive probe to propagation losses,” *J. Opt. Soc. Am. B* **19**, 2403-2412 (2002).
 12. M. Qiu, B. Jaskorzynska, M. Swillo and H. Benisty, “Time-domain 2D modeling of slab-waveguide-based photonic-crystal devices in the presence of radiation losses,” *Microwave and Opt. Tech. Lett.* **34**, 387-393 (2002).
-

1. Introduction

Waveguides and other optical elements, such as ultra-small cavities and abrupt bends, based on photonic crystals, are promising candidates to implement miniature integrated optics. While it is generally desirable in integrated optics to make use of single-mode waveguides, such guides have various drawbacks when they rely on high-index contrast structures, be it photonic crystal or not. The main difficulty is to couple light into them from fibers or broader deep-ridge waveguides. They are also very sensitive to fabrication imperfections, in particular to roughness of the walls, that induces not only large propagation losses, but also unwanted reflection and polarization conversion as soon as the translation invariance is broken, e.g., at a bend. Hence, broader multimode waveguides have been considered, with the idea of information transport in their fundamental mode. A typical example is the photonic crystal channel waveguides (PCCW) formed by three missing rows in a triangular lattice of holes etched through a vertically monomode semiconductor heterostructure (Fig. 1(a)), that we name W3 (Fig. 1(b)).

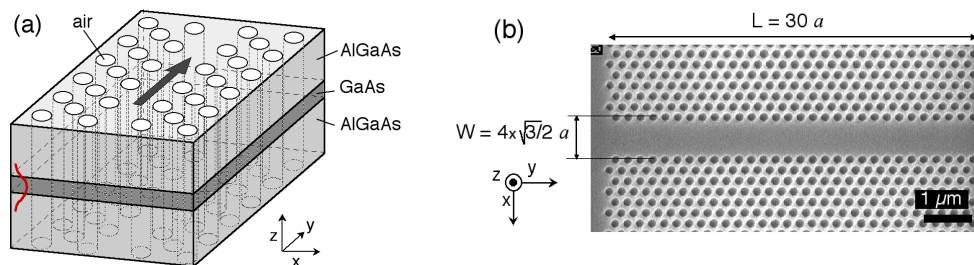


Fig. 1. (a) Two-dimensional photonic crystal etched through a vertically monomode semiconductor heterostructure ; (b) Micrograph of a three-missing-row PCCW (top view) with period $a=260$ nm in a GaAs heterostructure.

The periodicity of the photonic crystal waveguide boundaries is at the origin of Bragg coupling phenomena between guided modes, which occur at well-defined frequencies and wavevectors. In particular, the propagation of the fundamental mode is frustrated by diffraction induced by the corrugated boundaries, when its folded dispersion relation crosses that of a high-order mode with compatible symmetry [1,2]. Mode coupling is then manifested by a dip or mini-stopband (MSB) in the transmission spectrum of the fundamental guided mode and energy is transferred to the high-order mode, which propagates backward with larger losses. We prefer the term mini-stopband to minigap, because there is no cancellation of the overall density-of-states of the PCCW, due to the presence of other guided modes.

This phenomenon, specific to multimode PCCWs, could lead to an original coupling configuration between photonic crystal elements [3]. However its quantitative modeling has been, until now, numerical and relatively heavy, and for this reason, the impact of propagation losses could not be studied easily. We show in this contribution that an adequate generalization of the well-known coupled-mode theory, blended with plane-wave expansion simulations, now very classical for planar photonic crystals, results in simple and efficient modeling of these transmission mini-stopbands. We apply this analysis to the determination of propagation losses in three-missing-rows photonic-crystal waveguides W3, carved in a GaAs-based heterostructure.

2. Theory

2.1. Loss-less case

We consider a channel waveguide carved into a planar photonic crystal consisting of a triangular array of air holes etched through a semiconductor heterostructure by Reactive Ion

Etching (RIE). We focus here on canonical waveguides, i.e. defined by an integer number of missing rows, but any periodic line defect could be imagined (see [1,2]). Fig. 2(a) shows the dispersion relation of a three-missing-row waveguide calculated by the 2D plane wave expansion method in a supercell [4], where the vertical index structure is replaced by a homogeneous matrix, whose dielectric constant is taken as the square of the effective index of the vertical guided mode. The degree of validity of this 2D approach has been largely assessed [5]. For our GaAs-based heterostructure, the background dielectric constant is $\epsilon_{eff}=11$ and the air-filling factor is $f=0.37$, which leads to a photonic band gap in TE polarization covering the reduced frequency range $u=a/\lambda=0.22-0.3$.

The modes of W3 are easily classified and numbered by following the various branches: The fundamental mode, for which the scalar magnetic map $H_z(x,y)$ is represented in Fig. 2(c), basically resembles a traditional index-guided mode. Its dispersion relation is folded at the Brillouin zone edge due to the periodicity. The high-order modes follow at higher frequencies. The highest modes #4, #5 and #6, which have their cut-off frequency inside the photonic bandgap of the crystal, are purely Bragg-guided modes. They have a very low group velocity (or high group index $n_g=c/v_g$) when they cross the lower-order modes. If symmetry allows, anti-crossings instead of crossings occur between modes of different order, labeled “a” and “b”, when they obey the first-order Bragg condition: $\beta_a^0 + \beta_b^0 = 2\pi/a$ [1], giving rise to a mini-gap. As an example, Fig. 2(b) shows the local picture of the mini-gap associated to the coupling between mode #1 and mode #5, whose magnetic field patterns are represented in Figs. 2(c) and (d).

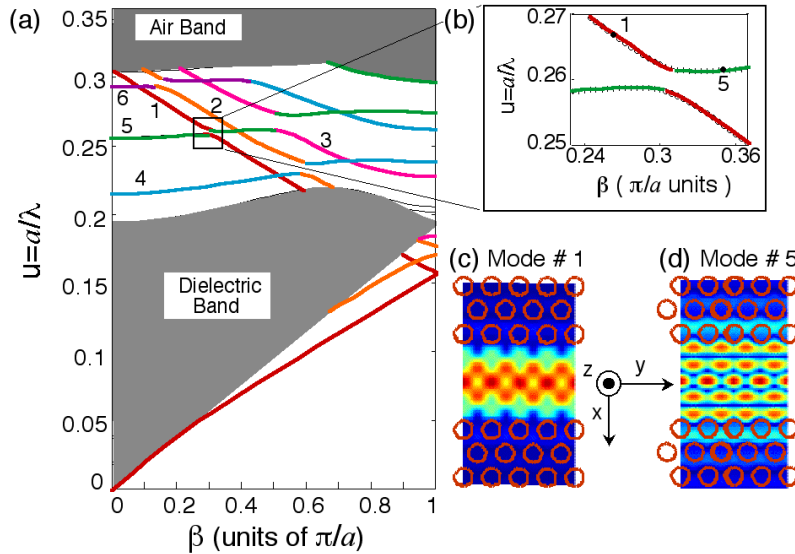


Fig. 2. (a) Dispersion relations of the W3 waveguide folded into the first Brillouin zone. The waveguide supports up to 6 modes ; (b) Local picture of the mini-gap associated to the coupling of the index-guided fundamental mode and the Bragg-guided 5th order mode ; (c)-(d) magnetic field patterns associated to the fundamental mode and to the 5th order mode.

We model the coupling of these two modes, around the central reduced frequency u_0 of the anticrossing, by the apparently classical coupled-mode formulation :

$$\frac{d}{dy} \begin{pmatrix} A(y, u) \\ B(y, u) \end{pmatrix} = \begin{pmatrix} -i\delta_a(u) & -i\kappa_{ab} \\ i\kappa_{ab} & i\delta_b(u) \end{pmatrix} \begin{pmatrix} A(y, u) \\ B(y, u) \end{pmatrix} \quad (1)$$

In this equation, $A(y,u)$ and $B(y,u)$ are the amplitude of both modes “a” and “b” along the waveguide and κ_{ab} is their coupling constant. $\delta_a(u)$ and $\delta_b(u)$, which are the detuning of the uncoupled modes with respect to the Bragg condition, can be expressed as a function of the reduced frequency u , assuming that the dispersion relations of the uncoupled modes are linear around the central frequency u_0 (i.e., their group velocities or group indices n_{ga} and n_{gb} are constant) :

$$\delta_a(u) = \beta_a^0 - \beta_a(u) = \frac{2\pi}{a} n_{ga} (u_0 - u) \quad (2a)$$

$$\delta_b(u) = \beta_b^0 - \beta_b(u) = \frac{2\pi}{a} n_{gb} (u_0 - u) \quad (2b)$$

The electromagnetic basis for such Eqs. is the same as the usual coupled mode equations introduced by Kogelnik [6,7]. Although they have widely been used in guided optics to describe the Bragg reflection occurring e.g. in distributed feedback lasers consisting in monomode corrugated waveguides, there have been few significant reports of their use to describe coupling between modes with very different group velocity. Multimode corrugated waveguides have been addressed in [8,9], but the authors have not considered in particular the role of the diminished group velocity of the high-order mode.

The resolution of the coupled Eqs. (1) leads to the analytical expression of the amplitudes of both modes along the guide, at any given frequency u around u_0 . In particular, they lead to the transmission spectra of the fundamental mode “a” at the output of the waveguide and to the reflection of the high-order mode “b” at the input displayed in Figs. 3(a) and (b) (red and green curves, respectively). The transmission spectrum of the fundamental mode presents a mini-stopband associated to the mini-gap in the dispersion relations. On both sides of the MSB, secondary oscillations characteristic for a Bragg diffraction phenomenon are observed. The spectral width Δu_{ab} of the minigap is equal to the frequency spacing between the first two maxima aside the dip in the transmission spectrum of the fundamental mode, when the length of the waveguide is infinite. It is related to the coupling constant κ_{ab} following the expression :

$$\Delta u_{ab} = \frac{a}{2\pi} \frac{4\kappa_{ab}}{n_{ga} + n_{gb}} \quad (3)$$

In practice, we need not calculate explicitly the coupling constant from the overlap integral of the mode profiles. Rather, we calculate the dispersion relations of the guide of interest using the plane wave expansion method in a supercell [4] and extract the numerical value of the mini-gap spectral width using a sufficiently thin k-space mesh for a very good accuracy. The group indices n_{ga} and n_{gb} of both modes are extracted from the slope of their dispersion relation, taken far from the coupling region. The value of the coupling constant κ_{ab} can then be derived from the knowledge of these three parameters, using Eq. (3). For the W3 waveguide considered above, the parameters extracted from the dispersion diagram of Fig. 2 are $n_{ga}=3.3$, $n_{gb}=33$ and $\Delta u_{ab}=2.5 \cdot 10^{-3}$, leading to $\kappa_{ab}=0.14 a^{-1}$.

2.2. Influence of propagation losses

When coming to real waveguides, the propagation losses α_a and α_b of both modes must be taken into account, in order to obtain an accurate model of the shape and intensity level of the transmission spectrum. The high-order mode, which has a much lower group velocity and a much larger penetration in the guide boundaries, experiences much larger propagation losses than the fundamental mode, with a realistic ratio of $\alpha_b/\alpha_a = 10$. For short waveguides (typically 30 rows), the losses of the fundamental mode will have a negligible effect, whereas they will become more visible for longer waveguides. The impact of the propagation losses is therefore studied separately in the following, where simulations are performed for a W3 waveguide of length $60a$.

Taking into account the propagation losses only for the high-order mode with the value $\alpha_b=0.1 \mu\text{m}^{-1}$, one obtains the spectra represented in Figs. 3(a) and (b), superimposed on the lossless spectra. The transmission and reflection spectra are essentially the bottom envelope of the spectrum calculated in the lossless case, washing out secondary oscillations. The transmission level of the fundamental mode still drops to zero at the central frequency, while the reflection of the high-order mode at the input is now well below 100 %.

Adding now the propagation losses of the fundamental mode with a smaller value $\alpha_a=0.01 \mu\text{m}^{-1}$, we obtain the spectra displayed in Figs. 3(c) and (d). The transmission of the fundamental mode at the output is 70 %, while the reflection level of the high-order mode at the input is essentially dominated by its propagation losses and suffers negligibly from the losses of the fundamental mode that excited it.

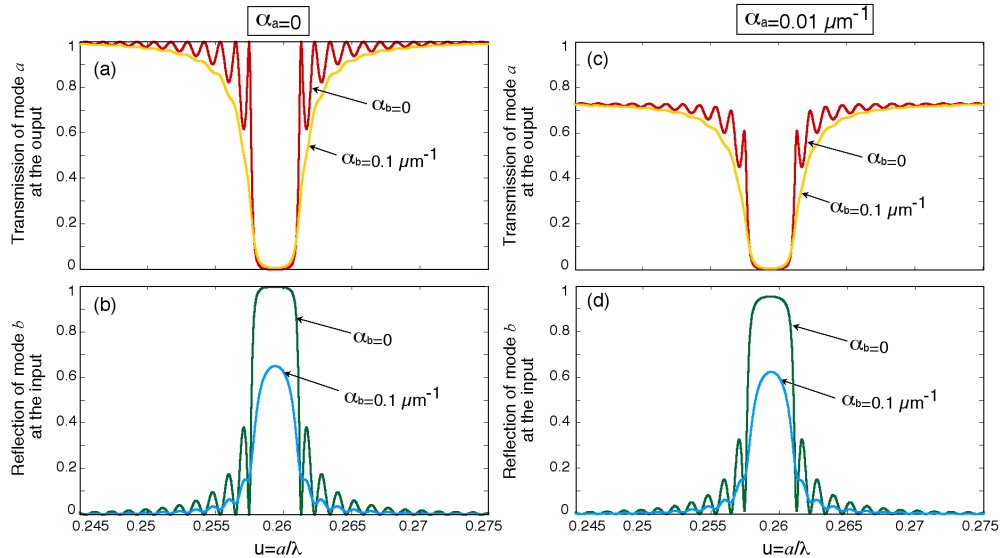


Fig. 3. Influence of the propagation losses on the spectral shapes of the transmission spectrum of mode a at the output of the guide and of the reflection spectrum of mode b at the input of the guide, showing the disappearance of secondary lobes.

3. Experimental results and comparison with theory

3.1 Experimental procedure

Three W3 waveguides of different length $60 a$, $120 a$ and $240 a$ (with $a=260 \text{ nm}$), carved into a GaAs-based heterostructure have been measured using the internal source technique described in earlier work [10] and illustrated in Fig. 4(a). The photoluminescence of InAs quantum dots embedded in the GaAs core of the heterostructure is used as an internal source to probe a photonic crystal structure. The source is created at the entrance of the waveguide at the focus of a laser diode and a spectral analysis of the signal collected at the cleaved edge after propagation through the PCCW is performed. Owing to the small internal collection angle dictated by the numerical aperture of the collection objective, the transmission of the fundamental mode is *selectively* measured, whatever the other excited guided modes.

3.2 Determination of the propagation losses

Figure 4(b) shows the experimental spectra. A MSB is observed around the frequency $u_0=0.265$, in good agreement with the frequency of the anticrossing in the dispersion diagram of Fig. 2. Note that the shift of the mini-stopband frequency towards the higher frequencies when the guide length increases is mainly an artefact due to the proximity effects during e-

beam patterning (slightly larger holes for larger overall exposure area). From the fit of the three experimental spectra with the coupling constant κ_{ab} and the losses α_a and α_b as the adjustable parameters, we obtain an accurate measurement of the losses of the fundamental mode and of the 5th order mode. We find $\alpha_a = 35 \text{ cm}^{-1} = 1.5 \text{ dB}/100 \mu\text{m}$ for mode #1 and $\alpha_b = 400 \text{ cm}^{-1} = 17 \text{ dB}/100 \mu\text{m}$ for mode #5, with an accuracy of 10%. The value of the coupling constant is $\kappa_{ab} = 0.09 a^{-1}$, a little below the calculated value $0.14 a^{-1}$, maybe on account of a minute width variation along the guide. It is remarkable that the spectral width of the transmission dip, simultaneously with the transmission level of the fundamental mode on both sides of the dip, are very well reproduced by the model. The propagation losses of the high-order mode are responsible for the apparently surprising fact that the MSB takes a broader and broader appearance when the length of the waveguide increases, whereas the coupling coefficient is unchanged.

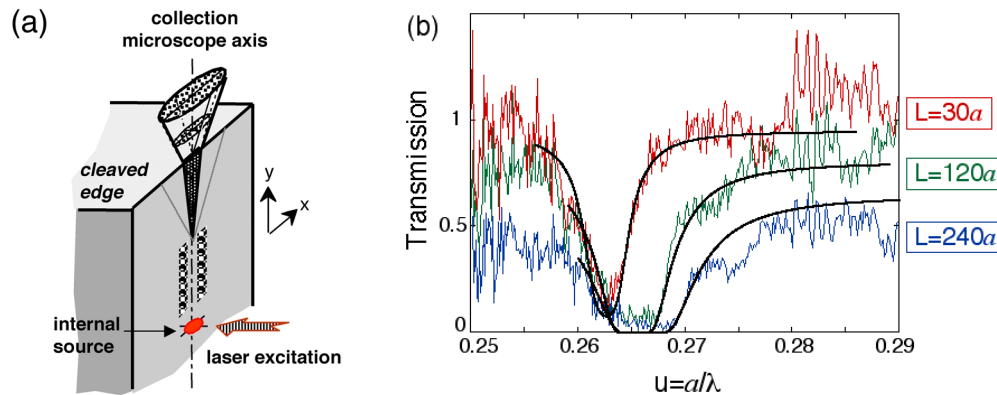


Fig. 4. (a) Experimental set-up for the selective measurement of the transmission of the fundamental guided mode ; (b) Experimental transmission spectra for W3 waveguides of lengths indicated on the graph (coloured curves) and fit using the coupled-mode theory (black curves) with the propagation losses as the only adjustable parameters.

3.3 Comparison with other methods

These propagation loss values have been cross-checked using a completely different method that our group has recently proposed [11]. This alternative method is based on the generation of the third guided mode by the deliberate insertion of constrictions at both guide ends: the interference fringes induced between third and fundamental modes are then used to retrieve modal propagation losses. Specifically, a loss value of 25 cm^{-1} for the fundamental mode of a W3 waveguide, similar to the one studied above (same hole diameter, period and, being fabricated by RIE, same depth as well), has been found using this alternative method.

4. Conclusion

We have assessed the validity of the coupled-mode theory to describe coupling between guided modes of very different nature and velocity in multimode photonic crystal waveguides, such as the index-guided fundamental mode and a low-group-velocity Bragg-guided mode. The coupled-mode theory, combined with the calculation of the dispersion diagram to extract the characteristic guided mode parameters, is a very powerful tool to fully describe the mode coupling phenomenon. It allows an excellent fit of the experimental data and therefore represents a very efficient and accurate tool to determine the propagation losses of the guided modes, compared to the time-consuming FDTD method, where the losses are taken into account in 2D in a model of dissipative air holes [12]. It is hoped that many photonic crystal devices and related phenomena can be described by extensions of the present work. We also

hope it could prompt three-dimensional full-vectorial simulations that would precisely establish the validity domain of the dissipative air holes.